Photoionization

T. R. Kallman[1]

[1]NASA Goddard Space Flight Center, LHEA, Code 665, Greenbelt, MD 20771

Photoionization Physics

- Photoionization = ionization of an atom or ion by a photon
- Just another ionization process ... but it can have important implications for the observed spectrum.
- Ionization rates (per ion):

$$\gamma_i \equiv \int_{\varepsilon_{Th}}^{\infty} F_\varepsilon \sigma_i(\varepsilon) \frac{d\varepsilon}{\varepsilon}$$

  F_ε= local mean intensity of radiation=$\frac{L}{4\pi R^2} f_\varepsilon$

  L=luminosity of radiation source

  R=distance to source

  f_ε=shape of spectrum such that $\int f_\varepsilon d\varepsilon = 1$

  $\sigma_i(\varepsilon)$=photoionization cross section

- A very simple approximation:

$$\sigma(\varepsilon) = \sigma_0 \left(\frac{\varepsilon}{\varepsilon_{Th}}\right)^{-3}$$

$$(\varepsilon \geq \varepsilon_{Th})$$

  where

$$\sigma_0 = \frac{2^8\pi}{3e^4}\alpha\pi a_0^2 = 6.3 \times 10^{-18}\mathrm{cm}^2 Z^{-2} n^2$$

$$\varepsilon_{Th} = 13.6\mathrm{eV} Z^2 n^{-2}$$

- A more accurate expression:

$$\sigma(\varepsilon) = \sigma_0 \left(\frac{\varepsilon_{Th}}{\varepsilon}\right)^4 \frac{e^{4-4\tan^{-1}(\eta)/\eta}}{1-e^{-2\pi/\eta}}$$

$\eta = \sqrt{\frac{\varepsilon}{\varepsilon_{Th}} - 1}$
for multi-electron atoms, need a numerical calculation.

Scaling behavior

- Rewrite the photoionization equilibrium equation:

$$n_e n_i C_i(T) + \frac{L}{4\pi R^2} n_i \int_{\varepsilon_{Th}}^{\infty} f_\varepsilon \sigma_i(\varepsilon) \frac{d\varepsilon}{\varepsilon} = n_e n_{i+1} \alpha_i(T)$$

$$\frac{n_i}{n_{i+1}} = \frac{\alpha_i(T)}{C_i(T) + \frac{L}{n_e 4\pi R^2} \int_{\varepsilon_{Th}}^{\infty} f_\varepsilon \sigma_i(\varepsilon) \frac{d\varepsilon}{\varepsilon}}$$

- The right hand side depends on atomic constants, temperature, f_ε (the spectrum shape), and $\frac{L}{n_e R^2} \equiv \xi$ known as the ionization parameter.

- Common definitions include:

  - $\xi \equiv \frac{L}{n_e R^2}$ (Tarter, Tucker and Salpeter 1969)
  - $U_1 \equiv \frac{N}{n 4\pi R^2 c}$ (Davidson 1974)
  - $\Gamma \equiv \frac{L_\varepsilon|_{13.6eV}}{n 8\pi R^2 c}$ (Kwan and Krolik 1981)
  - $\Xi \equiv \frac{L}{4\pi n_e ckT R^2}$ (Krolik, McKee and Tarter 1982)
  - $U_x \equiv \frac{N_X}{n 4\pi R^2 c}$ (Netzer 1994)

    where

    $N \equiv \int_{13.6eV}^{\infty} L_\varepsilon \frac{d\varepsilon}{\varepsilon}$

    $N_X \equiv \int_{100eV}^{\infty} L_\varepsilon \frac{d\varepsilon}{\varepsilon}$

    $L \equiv \int_{13.6eV}^{\infty} L_\varepsilon d\varepsilon$

Thermal Balance

- Photoionzation has the feature that we observe (in principle) the photons responsible for ionization and the photons produced by the gas, so it can be self consistent in the sense that it does not necessarily rely on an unobserved source of heat or ionization.
- If so, heat input from the source of illumination balances cooling by emission of reprocessed radiation.
- Heating is caused by:
  - Photoionization produces an electron with kinetic energy $\varepsilon - \varepsilon_{Th}$:

$$H_{PI} = \frac{L}{4\pi R^2} n_i \int_{\varepsilon_{Th}}^{\infty} d\varepsilon f_\varepsilon \sigma(\varepsilon)$$

  - Compton scattering produces electron with recoil:

$$\langle\frac{\Delta\varepsilon}{\varepsilon}\rangle = \left(\frac{4kT}{m_e c^2} - \frac{\varepsilon}{m_e c^2}\right)$$

$$H_{Comp} = \frac{L}{4\pi R^2} n_e \sigma_{Th} \int_{\varepsilon_{Th}}^{\infty} d\varepsilon \langle\frac{\Delta\varepsilon}{\varepsilon}\rangle f_\varepsilon$$

- Cooling is caused by any process with removes energy from the electron bath:
  - Recombination

$$C_{rec} = n_{i+1} n_e \alpha_i(T)(\varepsilon_{Th} + kT)$$

  - Collisional excitation/ionization

$$C_{coll} = n_i n_e C_i(T) \Delta\varepsilon$$

  - Compton scattering is included as a subtraction from the heating
  - Free-free emission

$$C_{ff} = n_i n_e \kappa(T) kT$$

- The thermal equilibrium equation can be written:

$$H_{PI} + H_{comp} = C_{rec} + C_{coll} + C_{ff}$$

where the terms on the left hand side are all proportional to L/R^2, and the terms on the right hand side are all proportional to n_e. So the temperature also depends on ξ.

Ionization and Thermal Balance Results

- Figures 1 and 2 show ionization and thermal balance results for an optically thin gas illuminated by a power law radiation field with $f_\varepsilon \sim \varepsilon^{-1}$.

- The mean ion stage is a monotonically increasing function of ionization parameter.

- Higher Z elements are more difficult to ionize than lower Z elements, so they survive against ionization to higher ionization parameter. At the highest ionization parameter, the most abundant ions are those from the heaviest elements.

- At $\log(\xi) \geq 5$ the gas is almost fully ionized. At $\log(\xi) \leq$ -3 the gas is almost fully neutral.

- Some ions are fragile, and essentially never occur as a pure charge state. Examples are ions with one electron outside a filled shell: Li-like, B-like, and Na-like.

- The gas temperature increases monotonically with ξ.

- At high ξ the temperature is determined primarily by Compton scattering. The "Compton temperature" depends only on the mean photon energy (for non-relativistic photon energies and temperatures), $T_{IC} = \frac{\langle\varepsilon\rangle}{4k}$, where $\langle\varepsilon\rangle$ is the mean photon energy. For many plausible spectra, such as $f_\varepsilon \sim \varepsilon^{-1}$, $T_{IC} \simeq 10^7 - 10^8$K.

- At low ξ the temperature is $\sim 10^4$K, determined by cooling by H I, He I, and other neutrals.

- T_{IC} depends on the steepness of the spectrum: Steeper spectra result in lower T_{IC}, and less ionization of ions with high ionization potentials at a given value of ξ.

- Compared with the coronal case, the temperature is much lower for a given ionization state, ie. $T \sim 0.1\langle\varepsilon_{Th}\rangle$, where $\langle\varepsilon_{Th}\rangle$ is the mean ionization potential of the most abundant ions in the gas.

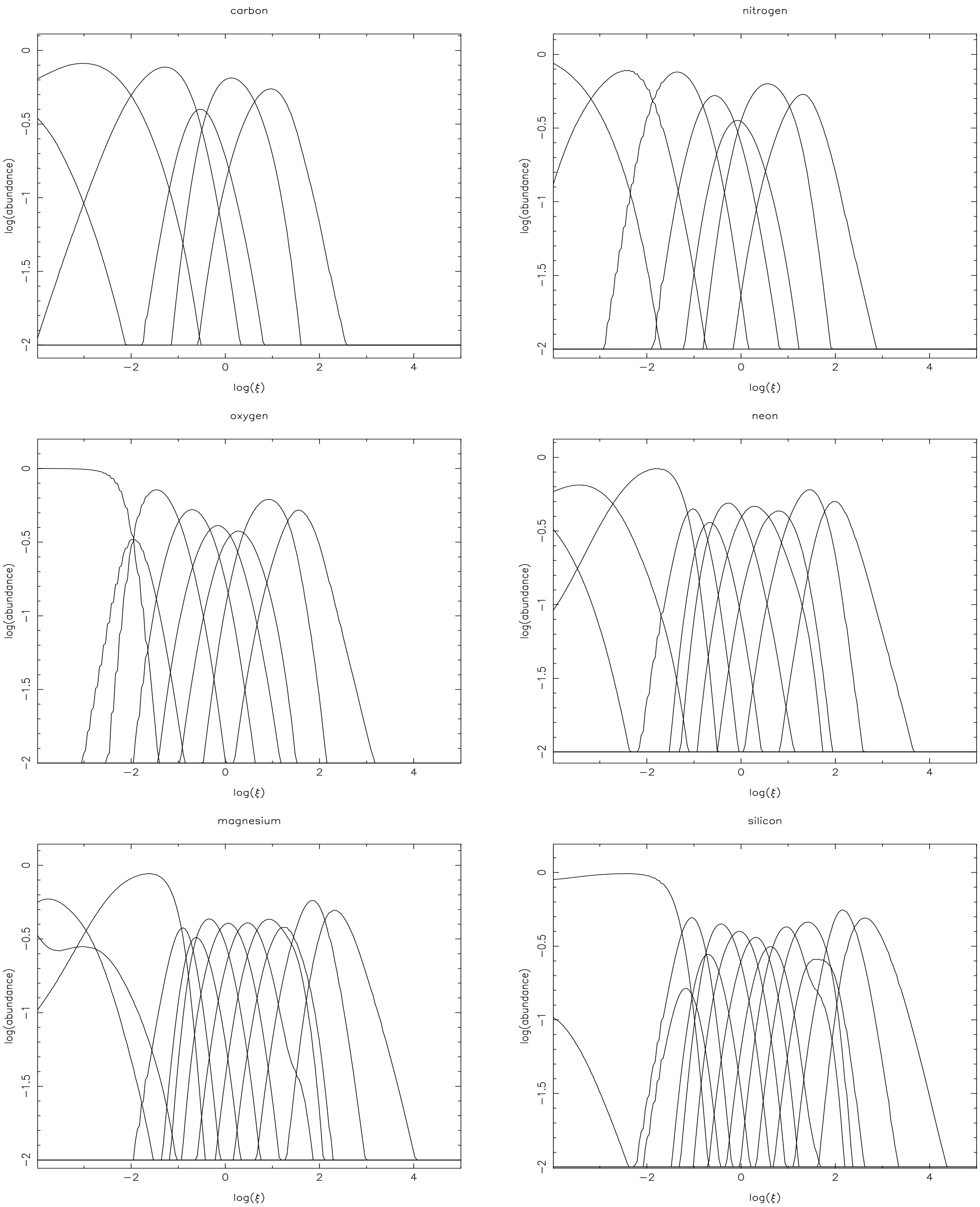
carbon
nitrogen
oxygen
neon
magnesium
silicon
log(abundance)
log(ξ)

Fig. 1.—

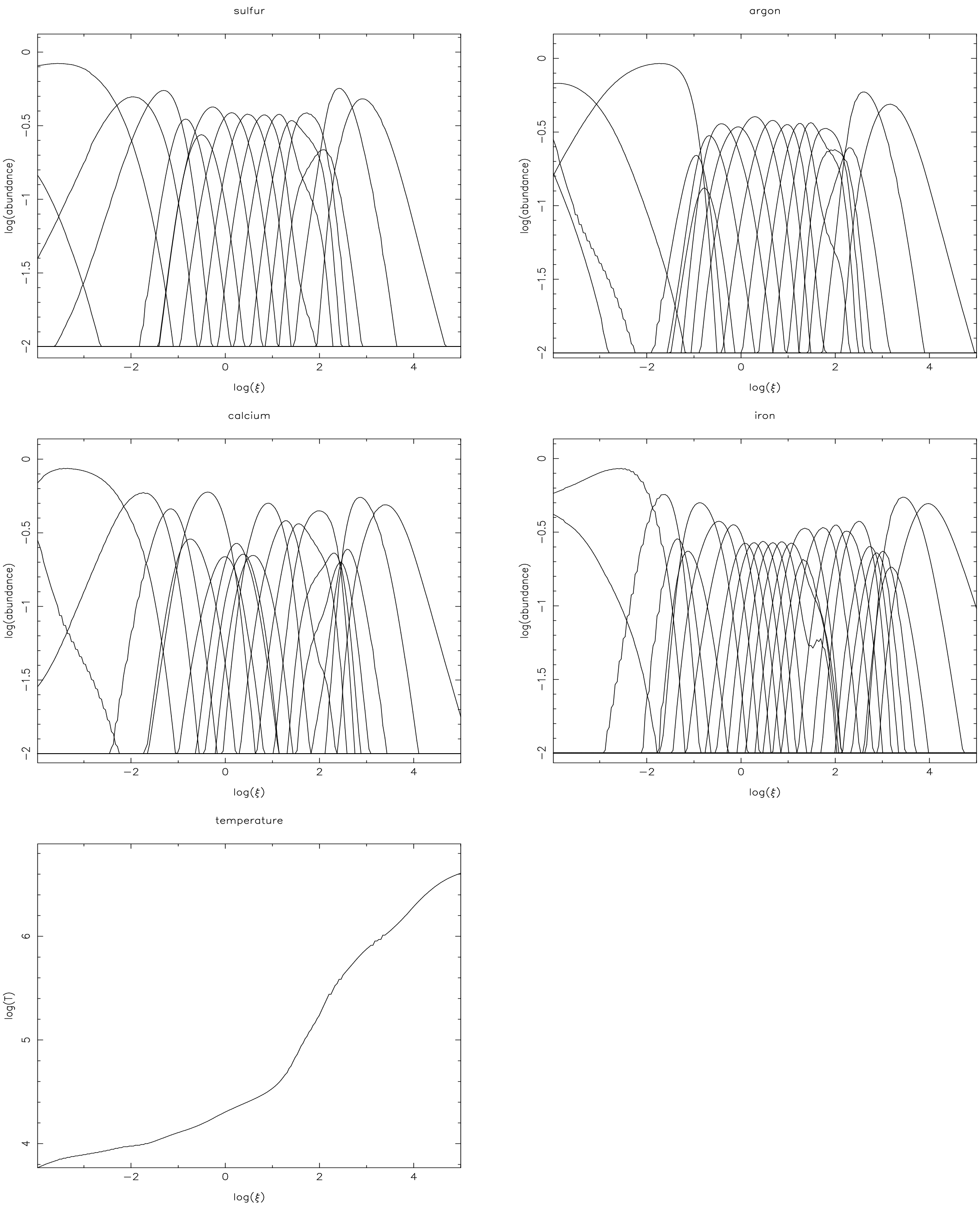
sulfur
argon
calcium
iron
temperature
log(abundance)
log(ξ)
log(T)
0
−0.5
−1
−1.5
−2
−2
0
2
4
6
5

Fig. 2.—

Thermal Instability

- The net cooling function of gas at constaant density can be written $\Lambda(T)$.
- If $d\Lambda/dT < 0$ the gas is thermally unstable. Perturbations in temperature will lead to a thermal runaway, which will be terminated only when the temperature reaches a range where the cooling function is stable.
- In order to assess thermal instability it is necessary to specify which other state variables are held constant when $d\Lambda/dT$ is evaluated. Examples are isobaric (constant pressure) and isochoric (constant density) variations.
- Gas which is stable to isochoric perturbations may not be stable to isobaric perturbations.

$$\left(\frac{d\Lambda}{dT}\right)_P = \left(\frac{d\Lambda}{dT}\right)_n - \frac{\Lambda}{T}$$

$$\left(\frac{d\mathrm{log}\Lambda}{d\mathrm{log}T}\right)_P = \left(\frac{d\mathrm{log}\Lambda}{d\mathrm{log}T}\right)_n - 1$$

  So gas with $\left(\frac{d\mathrm{log}\Lambda}{d\mathrm{log}T}\right)_n < 1$ will be unstable to isobaric perturbations.

- In photoionized gas, $\left(\frac{d\mathrm{log}\Lambda}{d\mathrm{log}T}\right)_n < 1$ can occur when the cooling is due to bremmstrahlung ($\Lambda \sim T^{1/2}$). $\left(\frac{d\mathrm{log}\Lambda}{d\mathrm{log}T}\right)_n < 0$ can occur if the ionizing radiation field is deficient in soft photons.
- Thermal instability at constant pressure is a common feature if the Compton temperature is $\geq 10^7$K.
- If so, there are two stable solutions for temperature (near 10^4K and 10^7K) and a third intermediate solution which is thermally unstable. This has been proposed as a mechanism for allowing cool ($\sim 10^4$K) clouds to be confined by hot gas in the same region in eg. AGN (Krolik, McKee and Tarter, 1982).
- This is illustrated in figure 3.

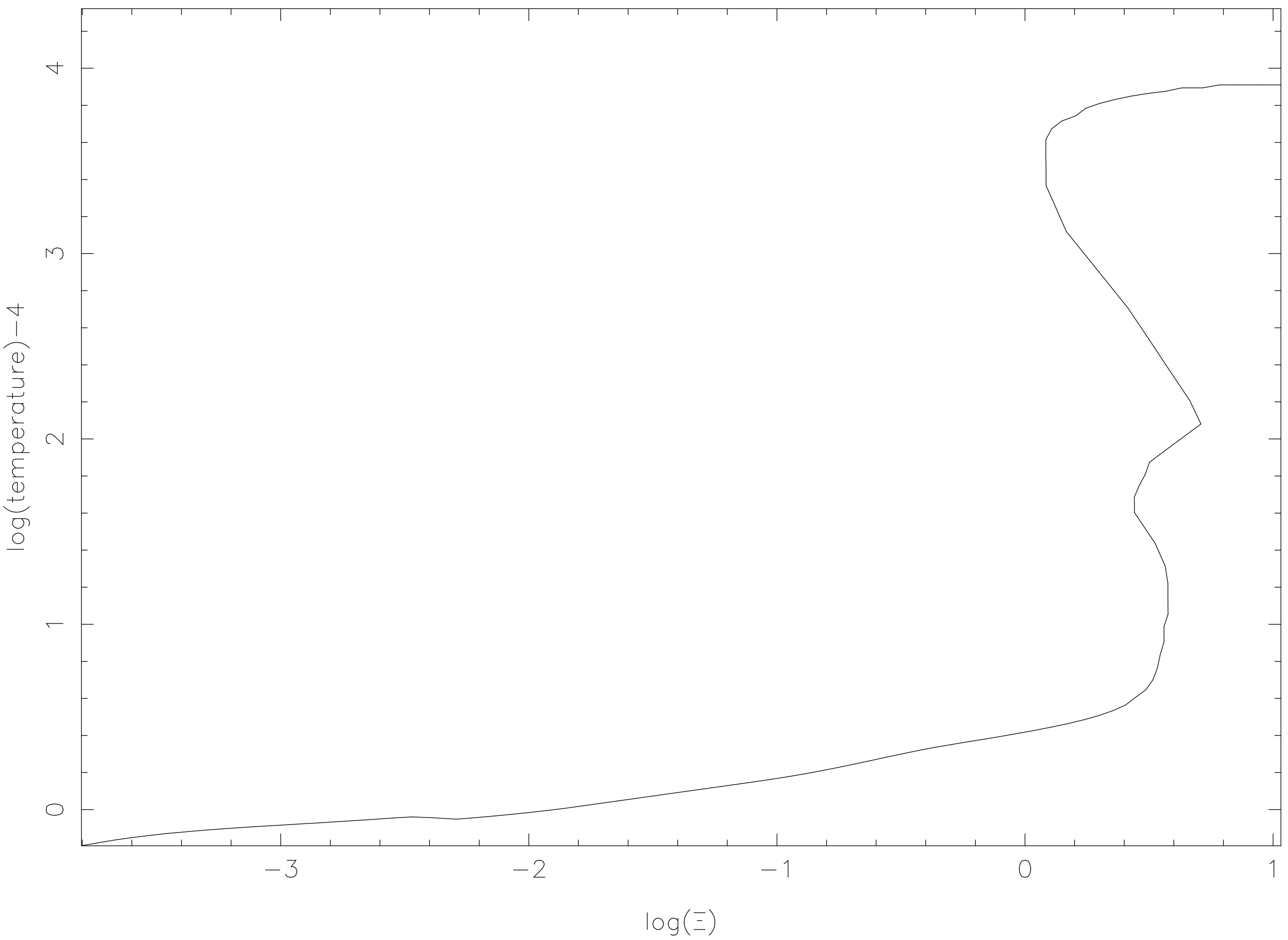

Fig. 3.—

Observable Effects I: Absorption

- If we substitute for ε_0 in the crude approximation for $\sigma(\varepsilon)$:

$$\sigma(\varepsilon) = \sigma_0 Z^4 \left(\frac{\varepsilon}{1\mathrm{Ry}}\right)^{-3} \quad \varepsilon \geq \varepsilon_0$$

- Now if we compare for various elements:

element	Z	abundance	$Z^4\times$abundance
H	1	1	1
He	2	0.1	1.6
C	6	10^{-4}	0.13
N	7	10^{-4}	0.24
O	8	10^{-4}	0.41
Ne	10	10^{-4}	1
Mg	12	10^{-5}	0.21
Si	14	10^{-5}	0.38
S	16	10^{-5}	0.66
Ar	18	10^{-5}	0.1
Fe	26	10^{-5}	4.6

- This shows that:
  - The cross section at threshold are all comparable: There are no large jumps in the total cross section for absorption by neutral material with cosmic abundances.
  - A corollary, then, is that any large edges whigh are detected suggest the existence of departures from this picture:
    * Partial ionzation, which can suppress the low Z elements (such as H and He) and thereby increase the prominence of the inner shell features of medium and high Z elements.
    * Or large departures from cosmic abundances.

- A crude approximation to the interstellar opacity is:

$$\sigma\varepsilon \simeq 1.5 \times 10^{-21} \left(\frac{\varepsilon}{1\mathrm{keV}}\right)^{-3}$$

Observable Effects Ib: Warm Absorbers

- A crude approximation for the photoionization cross section:

$$\sigma(\varepsilon) = \frac{\sigma_0}{Z^2}\left(\frac{\varepsilon}{\varepsilon_0}\right)^{-3} \varepsilon \geq \varepsilon_0$$

$$\sigma(\varepsilon) = 0 \mathrm{otherwise}$$

  where $\sigma_0 = 6.3 \times 10^{-18}\mathrm{cm}^{-2}$ is the threshold cross section for hydrogen, $\varepsilon_0 = 13.6Z^2\mathrm{eV}$ is the energy at threshold and Z is the ion charge.

  This shows that:

  - The cross section above threshold decreases as $\sim \varepsilon^{-3}$.
  - The threshold cross section decreases as $\sim Z^{-2} \sim \varepsilon_0^{-1}$.

- With a net result that higher charge cross sections dominate at high energies. An example is the inner shells of ions with more than ∼3 electrons. An example is shown in figures 4 and 5, which shows the cross sections for all ions of the 11 most abundant elements as a function of photon energy.

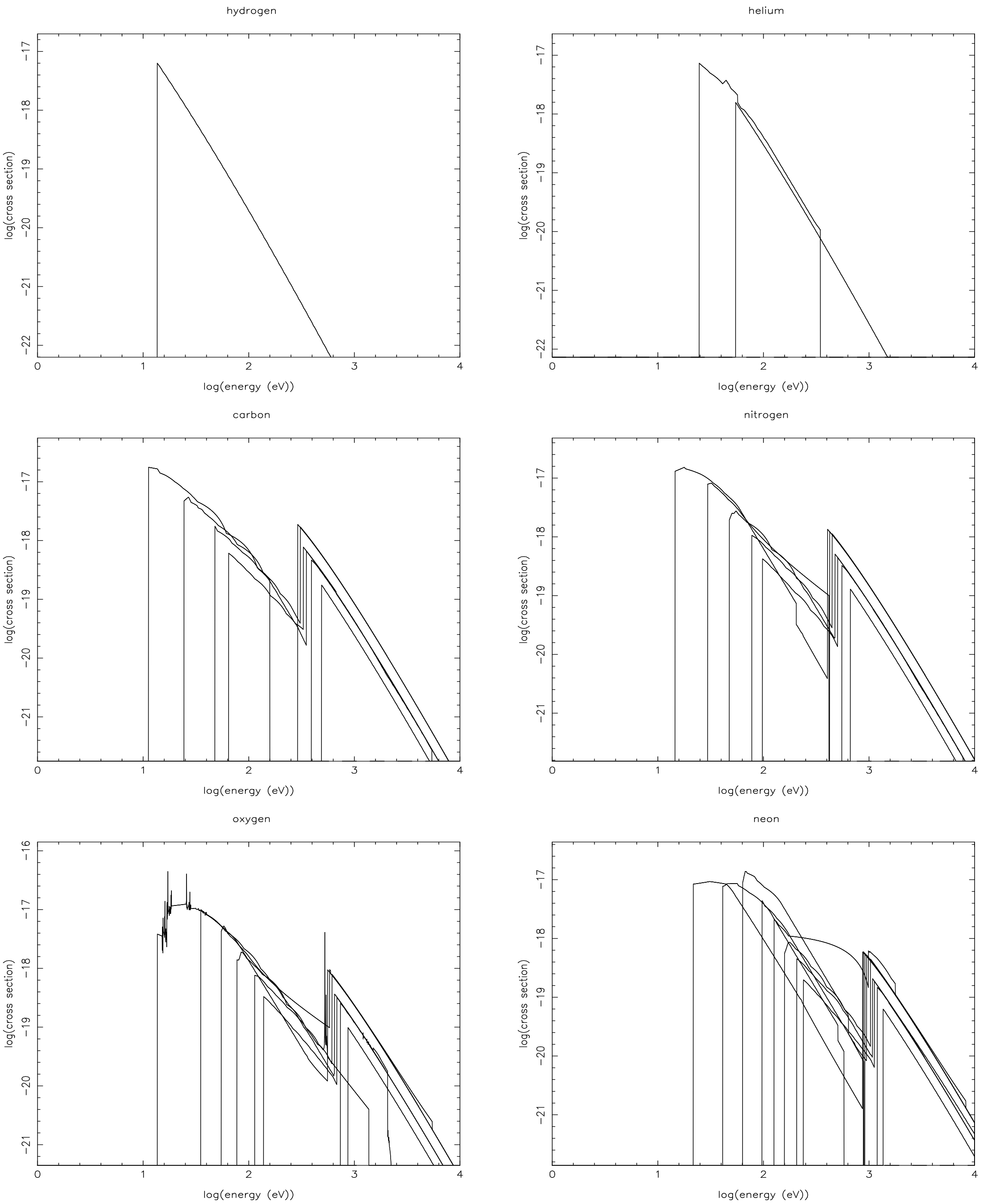
hydrogen
helium
carbon
nitrogen
oxygen
neon
log(cross section)
log(energy (eV))

Fig. 4.—

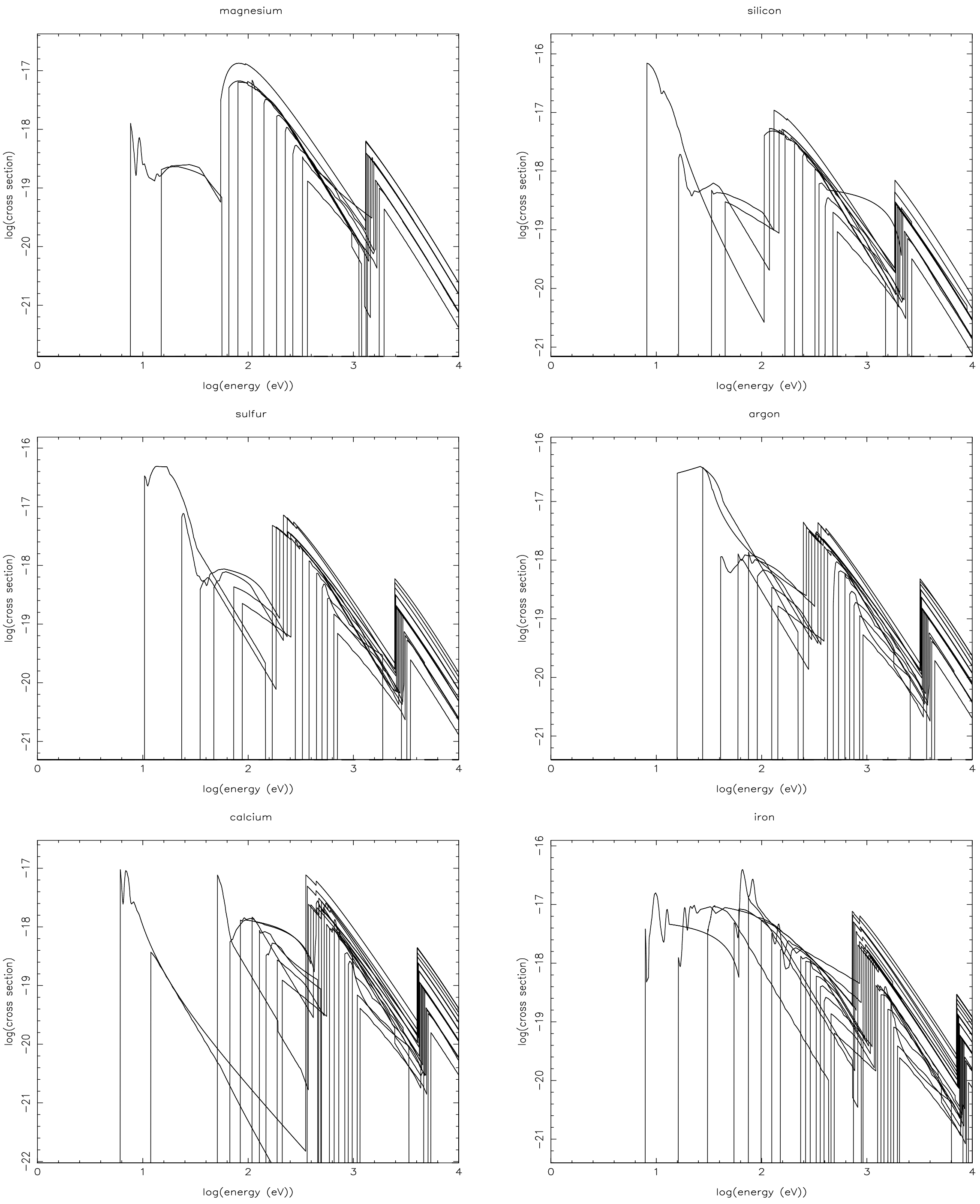
magnesium
silicon
sulfur
argon
calcium
iron
log(cross section)
log(energy (eV))
−16
−17
−18
−19
−20
−21
−22
0
1
2
3
4

Fig. 5.—

Observable Effects II: Emission

- Collisional excitation is less important than for coronal plasmas since kT$\leq 0.1\varepsilon_{Th}$. It is important only for lines close to ground, for example the 2s – 2p transition in Li-like ions.

- Recombination cascades are generally the dominant line emission mechanism. Since the recombination rates for high n levels vary as $\alpha_n(T) \sim n^{-1}$ high n levels are important. The Lyman decrement is generally flatter than for coronal plasmas.

- Recombination favors high angular momentum states. This affects the strengths of lines such as, for example, the 2-1 transitions in He-like ions, by preferentially populating the S=1 (triplet) levels rather than the S=0 (singlet) levels.

- Fluorescence following inner shell ionization leads to formation of iron K lines.

Observable Effects IIb: Emission from He-like Ions

- He-like ions have 3 'lines':

  w= $1s^2(^1S)$ – $1s2p(^1P)$ ("Allowed" or "resonance")

  x,y= $1s^2(^1S)$ – $1s2p(^3P_{1,2})$ ("intercombination")

  z= $1s^2(^1S)$ – $1s2p(^3S)$ ("forbidden")

- We can define 2 ratios:

$$R = \frac{z}{x+y}$$

  and

$$G = \frac{x+y+z}{w}$$

  The ratio R is sensitive to density since the z line has the lowest rate for radiative decay. At sufficiently high densities collisions can move electrons from the upper level of this line to the 2^3P level, thereby boosting the x and y lines at the expense of w. The lines are also sensitive to the mechanisms populating the upper levels. If this is done by electron collisions from the ground state, then the energy required is greatest for the upper level of the w line. Then G is primarily a function of temperature, and

$$R = \frac{R_0(T)}{1 + n_e/n_c}$$

  where $R_0(T)$ is a function only of T and n_e is the electron number density and $n_c = \frac{\mathrm{A(^3S-^1S)}}{\mathrm{C(^3S-^3P)}}$ is the critical density for the collisional transfer between the 2^3S and the 2^3P levels.

- If the assumption of collisional population is correct, then using the 2 ratios it is possible to infer both T and n_e from measurements of the 3 lines w, $x+y$, and z.

- Complications:

  – Recombination increases G and R at low n_e

  – K shell Ionization of Li-like ions can also lead to emission of these lines

  – Resonance line scattering can affect the strength of the w line.

Observable Effects IIc: Iron K Lines

- Iron K lines are unique in that they can be emitted efficiently from gas ranging from neutral to highly ionized.

- The intrinsic line energy is a measure of ionization state. Absence of confusing lines from other species facilitates this measurement.

- Iron is more likely to survive against photoionization than other abundant elements in environments with high fluxes of ionizing radiation, but the apparent detection of near-neutral iron within $\sim$a few gravitational radii of a black hole in AGN is somewhat surprising.

- For ions with $\leq$10 electrons, measurements of the line energy and structure are likely to yield sensitive constraints on the gas ionization state, and possibly also gas motions, relativistic effects, and Compton scattering.

- Recombination continuum radiation accompanies lines formed by cascades. This is illustrated in figure 6, which shows the recombination spectrum of O VIII at 10^5K.

$$\text{Shape} \sim e^{-(\varepsilon-\varepsilon_{Th})/kT}$$

$\rightarrow$ width is a measure of T.

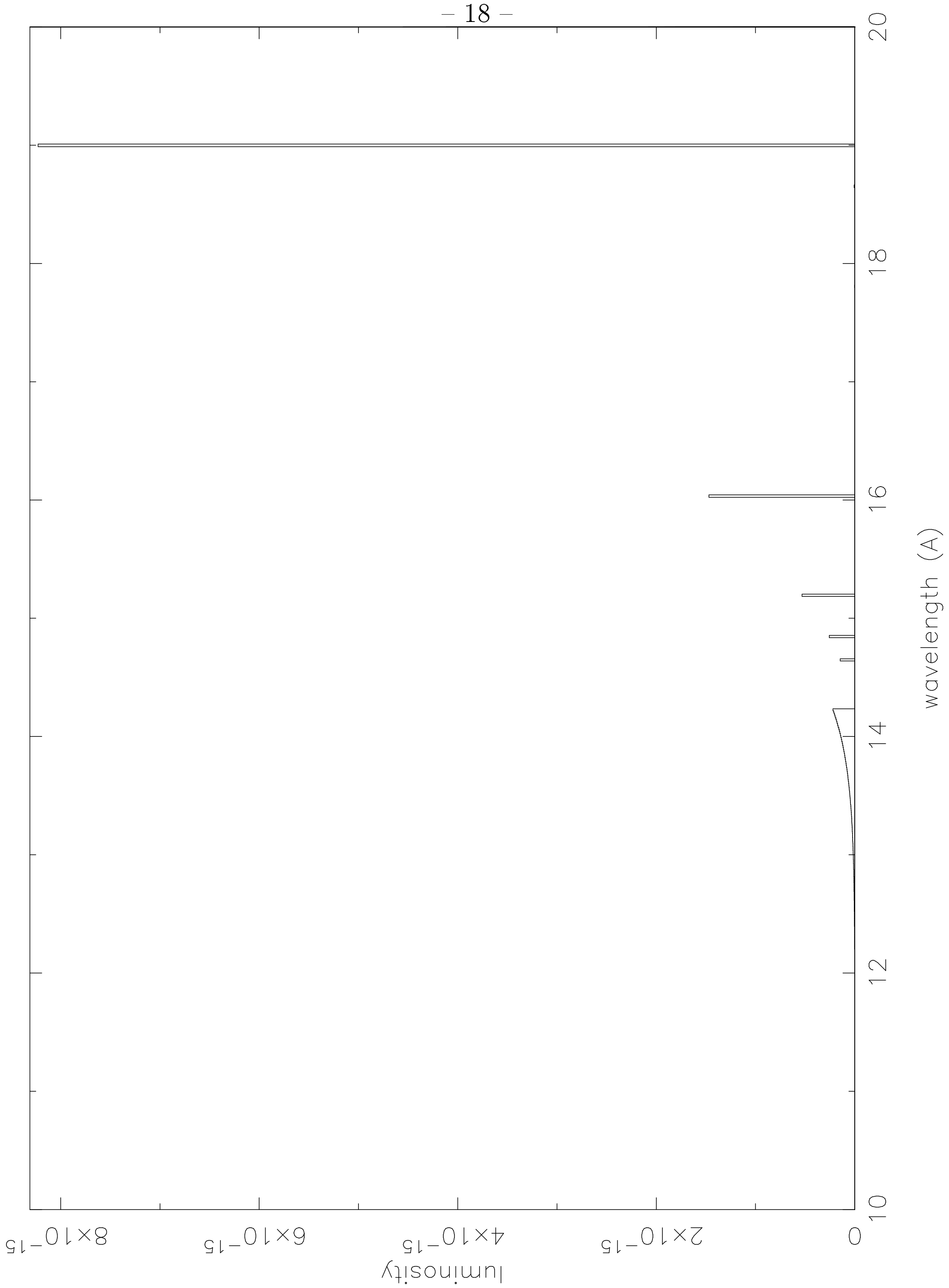
luminosity
0
2×10^{-15}
4×10^{-15}
6×10^{-15}
8×10^{-15}
wavelength (A)
10
12
14
16
18
20

Fig. 6.— a

Practical Issues

- Free parameters which may be important in specifying a model: ξ, f_ε, column density, 'geometry' (i.e. covering fraction, departures from spherical symmetry).
- Signatures of photoionization:
  - recobmination continua
  - He-like ratios (i.e. R, G ¿ 1)
  - Temperature
  - Flat Lyman decrement
- Available models, and where to go to learn more:
  - xstar

    `http://heasarc.gsfc.nasa.gov/docs/software/xstar/xstar.html`

    cf. Kallman and Bautista (2001)
  - cloudy

    `http://www.pa.uky.edu/~gary/cloudy/`
  - ion (Netzer)
  - apec

    `http://hea-www.harvard.edu/APEC/`
  - HULLAC (LLNL/Columbia)

REFERENCES

Davidson, K. 1974, ApJ, 218, 20.

Ferland, G. J.; Korista, K. T.; Verner, D. A. 1997a ASP Conf. Ser. 125: Astronomical Data Analysis Software & Systems VI 6, 213

Kallman, T., and Bautista, M., 2001, ApJ 133, 221

Kallman, T., and McCray, R., 1982, Ap. J. Supp., 50, 49

Krolik, J., McKee, C., and Tarter, C. B., 1981, Ap. J., 249, 422

Kwan, J. & Krolik, J. 1981 ApJ 250 478

Netzer, H., 1994, Ap. J. 411, 594

Tarter, C. B., Tucker, W, & Salpeter, E. 1969, ApJ, 156, 943